Design of Microstrip Patch H-Notch Antenna for Vehicle Using Array Systems

Raed S. M. Daraghma

Department of Telecommunication Technology Engineering, Faculty of Engineering and Technology, Palestine Technical University, Kadoorie (PTUK), Tulkarm, Palestine
Email: R.daraghmeh@ptuk.edu.ps (R.S.M.D.)

***Abstract*—The need for micro antennas is growing as Internet of Things (IoT) applications spread quickly in today's communication systems. Due of their interoperability, Microstrip patch antennas are frequently employed in Internet of Things (IoT) applications. The suggested antenna is made on a single side of high-quality Teflon substrate and has a small, dimension 17.19×17.8×0.933 mm^3; the antenna can be utilized for IoT applications because it is made to operate at a frequency of 5.9 GHz. It is made up of an array of H shapes and is intended to be integrated into an IoT gadget as integrated antenna. Thus, in this work, rectangular Microstrip Patch H-Notch antenna is designed and the performance was analysed. The antenna resonant frequency range was 5.9 GHz, which is appropriate for IoT applications. The antenna was designed with Teflon substrate material. For this work, Computer Simulation Technology (CST) software was used as simulation software. In this work, two types of antennae were designed, which was conventional Microstrip H-notch antenna and rectangular Microstrip antenna containing Array-shaped structure. The performance of these two antennas was compared in terms of bandwidth, gain and return of loss. The key results of this work showed that the optimized Array-shaped antenna improved the bandwidth, gain and return of loss compared to the conventional antenna. In addition, the optimized antenna achieved operating frequency of 5.9 GHz, which is suitable for IoT applications.**

***Keywords*—Microstrip Patch H-Notch, Internet of Things (IoT), Bandwidth**

I. Introduction

The so-called "5G" generation of mobile broadband networks promises more coverage, substantially faster data speeds, extremely low latency, and extremely stable connections for smartphones and other devices. For new smart service and application domains without involving human involvement, including vehicle-to-vehicle, machine-to-machine, Internet-of-Things (IoT), or Vehicle-To-Everything (V2X), sensors, servers' communications gateways, security cameras, autonomous cars, unmanned aerial vehicles, medical robots, etc., 5G will be essential to work alongside 3G/4G systems and coexist with Low Power Wireless Area (LPWA). Low-power, long-range radio modems are used by LPWA wireless networks to connect with Internet of Things devices in areas where cellular services are either unreliable or have inadequate coverage, like: rural regions, remote areas with inadequate coverage, places that are hard to get to and that make installing cellular towers challenging, Wearables and smart home appliances are two applications that benefit from LPWA networks since they use low-power batteries.

Akbar *et al*. [1] developed an orthogonally integrated hybrid antenna to handle 5G, Wi-Fi, and C-V2X connection concurrently. Three planar monopoles and a flawed ground plane with a size of 55×30×1.2 mm^3 make up the suggested antenna.

Alsariera *et al*. [2] proposed a new compact Circularly Polarized (CP) monopole antenna that feeds into a Coplanar Waveguide (CPW). The antenna structure consists of an L-shaped monopole, an asymmetric modified ground plane, and a few series-aligning inverted L-shaped strips.

Kumar *et al*. [3] presented Microstrip Patch antenna, the proposed antenna operates in two bands 1.5 GHz and 7 GHz with the later band being wideband, spanning the frequency range of 5.32 GHz to 8.27 GHz. In order to achieve the intended performance, different geometric parameters of the planned antenna have been changed.

In Ref. [4], a circular Microstrip patch antenna supplied by a CPW is suggested for use in ultra-wideband applications. The antenna's overall dimensions are 40×40 mm^2; it is constructed from a 1.6 mm thick FR-4 substrate with a dielectric constant of 4.4. The suggested antenna has two resonance frequencies at 1.6 GHz and 5.2 GHz and operates over a wide bandwidth that tends to cover the ultra-wideband of 1.2–7.2 GHz.

Singh *et al*. [5] investigated a multiband CPW-fed antenna's |S11| parameter. The proposed structure, which was built on FR4 substrate made of flame-resistant fiberglass epoxy, spanned a broad frequency range between 1.5 GHz, 3.2 GHz, 3.4 GHz, and 3.65 GHz.

Boontamchauy *et al*. [6] proposed an inverted L-shaped patch antenna, diagonally attached to a square branch, with a corner-truncated partial ground plane. The corner-truncated partial ground plane was employed to increase the Axial Ratio Bandwidth (ARBW), while the adjacent

Manuscript received November 1, 2023; revised December 1, 2023; accepted December 13, 2023; published April 17, 2024.

square branch was used to disturb linear polarization for circular polarization. The ARBW of the suggested antenna would be 77.87% (1.09–2.48 GHz).

Yoon [7] proposed a revolutionary design for a straightforward rectangular ring with open-ended monopole antenna WLAN applications. The suggested antenna was developed, made, and tested as prototypes. The proposed antenna, which receives frequencies between 2.3125 GHz, 2.775 GHz, 4.8625 GHz, and 6.7125 GHz with a return loss of less than −10 dB and fulfils the necessary bandwidths of the 2.4 GHz, 5.2 GHz, 5.8 GHz WLAN standards.

Hossain *et al.* [8] discussed a wideband patch antenna for head imaging based on Grounded Coplanar Waveguides (GCPW). A slotted inverted delta-shaped primary radiating patch, CPW elements, and a slotted partial ground plane are all combined into the proposed antenna. The simulation and measurement findings show that the suggested prototype exhibits almost directed radiation properties and a bandwidth of 2.01 GHz (1.70–3.71 GHz). The prototype has a maximum radiation efficiency of 93% over the frequency band and a maximum gain of 5.65 dBi.

Chiu and Chi [9] provided an internal multiband Inverted-F Antenna (IFA) for applications in mobile devices. The suggested antenna consists of two parasitic elements to increase bandwidth and a dual-band primary Inverted-F resonator. The operating bands can support GSM 900, DCS, PCS, UMTS 2100, WiMAX, Hyper LAN 2, and IEEE 802.11a/b/g.

Ma *et al*. [10] presented and analyses a Circular Coplanar Inverted-F Antenna (CCIFA) for UHF Machine-to-Machine (M2M) communications. The suggested antenna has a single metal layer that forms a ring and disc with a radius of less than 0.1 using a standard PCB. Analysis is done on a 480MHz optimized design with a 33mm radius.

Rahayu and Hidayat [11] covered single, two, four, and six element dual-band (28/38GHz) Microstrip antenna arrays for 5G applications. On a Rogers Duroid 5880 substrate with a thickness of 1.575 mm, a loss tangent of 0.0009, and a dielectric constant of 2.2, the suggested antennas are produced. They consist of a 50-Microstrip line feeding a triangle-shaped radiating patch. Maximum gain is 7.47 dBi at 28 GHz with a return loss of –30.70 dB, and maximum gain is 12.1 dBi at 38 GHz with a return loss of Rahayu, M. Hidayat 34.5 dB.

In Ref. [12], with the help of an innovative design, the new antenna proposed in this study can improve the performance level of IoT applications. The antenna was created, tested, and reviewed using simulations of actual operational conditions. Based on the results, it was determined that it will function well and be suitable for IoT applications that require the 868 MHz frequency spectrum. The authors discovered the best Microstrip patch antenna configuration with two notches along the x-axis, a reflection coefficient of 34.3 dB, and a bandwidth of 20 MHz

Katoch *et al.* [13] presented a tiny strip patch antenna with dual frequency functionality. The proposed antenna consists of a single rectangular Microstrip main patch and two slotted patches connected to the main patch. The antenna can be utilised for IoT applications. The antenna's measured gain without connecting patches is 4.4 dB, but when slotted patches are used to link it, the gain rises to 5.01 dB.

Santamaria *et al.* [14] described a slot-based Electrically Steerable Parasitic Array Radiator (ESPAR) antenna suitable for IoT applications. The antenna is capable of emitting radiation in 12 different directed and two slightly different omnidirectional states. With the aid of the 12 directional patterns, the antenna is able to concentrate the radiated energy in six distinct directions that are evenly distributed in the azimuth plane and have two different beam widths.

Simanjuntak *et al*. [15] employed an edge weight to design a planar Microstrip antenna with N elements (λ /2) evenly spaced apart. The 5G 2.6-GHz operating frequency will provide a multi-beam pattern with an antenna design that ranges from 1×3 to 1×6. Using a parasitic and a non-parasitic patch, each patch is separated by λ /2, and the value of S11 is less than -20 dB.

Rajesh *et al*. [16] discussed the design of a wearable antenna for 2.4–2.45 GHz and 5.7–5.85 GHz Industrial, Scientific, and Medical (ISM band) applications. Two sets of slots, one with the same length and the other with a variable length, are implemented for the rectangular Microstrip patch antenna. Copper and fabric are used to make the conductive and ground planes, respectively. In this instance, textile material acts as a barrier between the human body and the antenna while copper acts as a conductor. The radiation pattern, gain, VSWR, and reflection coefficient of Microstrip textile antennas, which are employed in many ISM band applications, are obtained in order to evaluate the performance of the antenna both theoretically and practically.

Alsudani and Marhoon [17] introduced an MP antenna and MP antenna array for 5G-based, 28 GHz applications using computer simulation technologies and antenna modelling tools. The mushroom-shaped Electromagnetic Band Gap (EBG), which is implanted with the MP antenna and MP antenna array in order to remove the presence of surface waves that have a detrimental impact on the antenna gain, is used to optimise and improve the simulated MP antenna characteristics. The simulation findings show that the gain is improved with the mushroom-shaped EBG to be 6.48 dBi and greatly with the array arrangement to be 11.9 dBi.

Many researchers have examined and assessed various kinds of antennas for vehicle communication. The survey addresses slot antennas, printed monopole antennas with multiband operations, and H notch antennas for a variety of vehicle applications, and it offers numerous solutions. Multiple frequency operation is possible with stacked antennas, and several monopole topologies were examined.

The simulation demonstrated that the aforementioned literature has presented a wide variety of IoT settings. Low fabrication costs, simplicity of integration with curved product or vehicle surfaces, ease of attaining both linear and circular polarization, and ease of design are some

advantages of these setups. Low impedance, narrow bandwidth, and environmental sensitivity to temperature and humidity variations are a few of their disadvantages. Along with the aforementioned limitations, the gain and efficiency of the antenna are also important in vehicle communication and can be increased by using Array H patch antenna.

Considering the prospects and potential for these study topics to be developed further, we still wish to investigate Certain strategies were integrated into the design of a typical Microstrip-H-patch antenna to ensure size reduction and improve bandwidth.

The antenna that is going to be installed on the exterior of the car needs to be tiny and lightweight. Consequently, the use of irregular ground planes with high permittivity substrate is advocated for antenna miniaturization; nevertheless, this approach is expensive and complex. A result of these effects, Array H Patch with low-profile is proposed.

CST simulator is used to design the different types of Array Patch antennas. The CST tool from ANSYS is used to design the antenna in this work. It is a 3-D, full-wave, electromagnetic solver. It contains the most recent solver technologies for applications that use microwave and radio frequencies, based on the finite element method, Maxwell's integral equation.

The major contribution of this paper includes:

- The innovative Microstrip patch antenna model was thoroughly investigated through in-depth parametric analysis to arrive at a final optimized antenna design for excellent impedance matching. It has a super tiny size of 17.119 mm×17.8 mm ×0.933 mm.
- Design an array and Microstrip patch antenna with a rectangular shape that may be used for vehicular applications while considering design considerations to optimize the various antenna parameters.
- Design a Microstrip patch antenna that is compact, light, and low manufacturing costs allow for large-scale production.

The following is how the paper is organized. Section II covers the general aspects of Microstrip patch antenna Design. Section III presents simulations and analysis of proposed antennas, as well as a diagrammatic comparison of different antennas. Section IV shows the results and discussions while Section V closed by conclusions.

II. Antenna Desgin

In order to calculate the length and width of antenna several equations are used.

The patch antenna's width is calculated using [18]:

$$W = \frac{c}{2f_0\left(\varepsilon_r + \frac{1}{2}\right)} \quad (1)$$

where c = 3×10^8 m/s, W: width of microstrip line, ε_r: relative dielectric constant of substrate, f_0: resonant frequency.

The effective length of patch depends on the resonant frequency (f_0) [18].

$$L_{eff} = \frac{c}{2f_0\sqrt{\varepsilon_{reff}}} \quad (2)$$

where

$$\varepsilon_{reff} = \frac{\varepsilon_r+1}{2} + \frac{\varepsilon_r-1}{2}\left[1+\frac{h}{w}\right]^{\frac{1}{2}} \quad (3)$$

Actual length and effective length of a patch antenna can be related as:

$$L = L_{eff} - 2\,\Delta L \quad (4)$$

$$\frac{\Delta l}{h} = 0.412\frac{\left(\varepsilon_{reff} - 0.3\right)\left(\frac{w}{h}+0.264\right)}{\left(\varepsilon_{ref} - 0.258\right)\left(\frac{w}{h}+0.8\right)} \quad (5)$$

where $\frac{\Delta l}{h}$ is a function of effective dielectric constant ε_{reff} and the width to height ratio $\left(\frac{w}{h}\right)$.

The planned antenna has a loss tangent (d) of 0.002 and is printed on a Teflon substrate with a thickness of 0.933 mm. Fig. 1 shows the prototype of the designed antenna and measurement set-up. The parametric study was used to determine the ground plane length, which is depicted in Fig. 1. At 5.9 GHz, the intended antenna operates. Applications for Wireless Access Vehicular Environment (WAVE) are the focus of this band. Table I discusses the parameter for antennas with the suggested work.

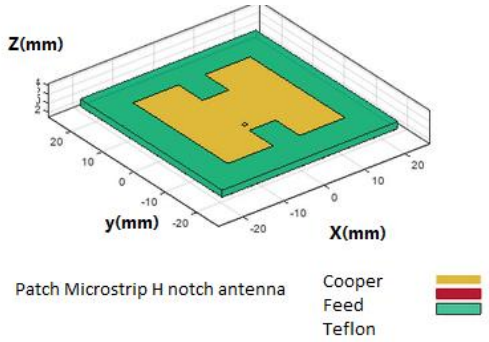

Fig. 1. Structure of desgined antenna.

TABLE I. Simulation Parameter

Parameter	Configuration
Length (mm)	17.19
Width (mm)	17.8
Notch Length (mm)	3.85
Notch Width (mm)	4.5
Height (mm)	0.933
Ground Plane Length (mm)	25.7
Ground Plane Width (mm)	26.6
Feed Diameter	0.59
Substrate type	Teflon
Epsilone	2.1
Loss Tangent	0.0002
Thkcness of substrate (mm)	0.933
Conductor Type	Copper
Conductivity (S/m)	59600000
Thikness of conductor (mm)	0.0035

III. Simulations and Analysis

A. Case I

Patch Microstrip H-notch antenna element as specification in Table I.

Fig. 2 displays the attributes of the suggested antenna.

There is only one resonance available for the simulated s-parameter (5.7 GHz–5.9 GHz). Fig. 2 displays the simulation's measured results for return loss. At 5.9 GHz, the return loss is −12 dB, and at 5.8 GHz, it is −14 dB. Additionally, we can see that the antenna performs at S11< −10 dB at 0.2 GHz (5.9–5.7 GHz).

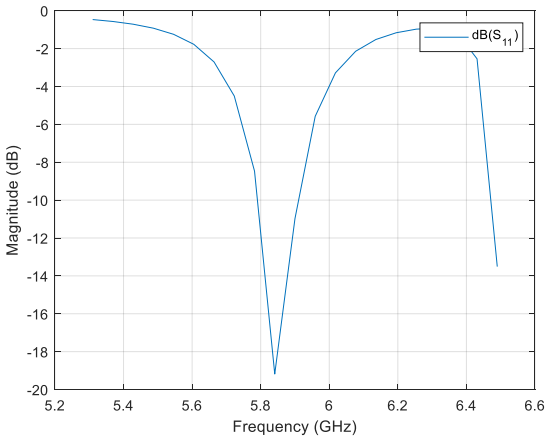

Fig. 2. Simulated S- parameter results.

The surface current distributions at 5.9 GHz are displayed in Fig. 3 in order to describe the UWB responses of the Patch micro strip H notch antenna. According to Fig. 3, the linearly tapered feeding line with a high current value is where the surface current is largely focused. It is observed that the current is not followed at the upper patch of the radiating patch at this resonance frequency of 5.9 GHz, acting as a frequency function. The suggested antenna's radiation patterns were measured and examined in Fig. 4. The gain value was around 7.015 dB.

Azimuth and elevation radiation patterns for Microstrip patch antennas operating at 5.9 GHz are shown in Fig. 5(a) and Fig. 5(b), respectively. The maximum gain of the antenna is around –3.359 dB in azimuth pattern and 7.015 dB in elevation pattern.

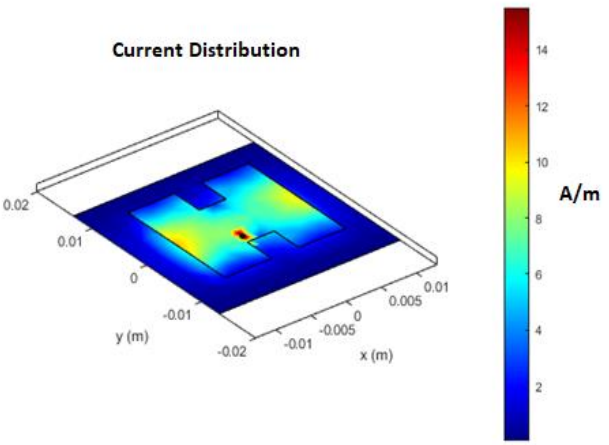

Fig. 3. Current follow concentrations at frequency 5.9 GHz.

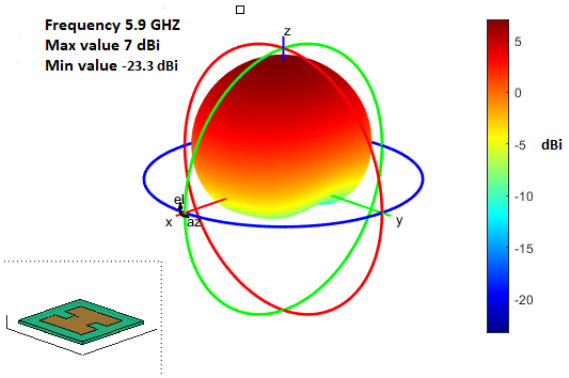

Fig. 4. 3D Radiation pattern.

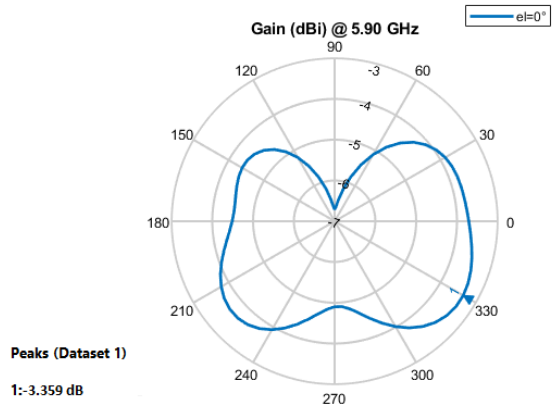

(a)

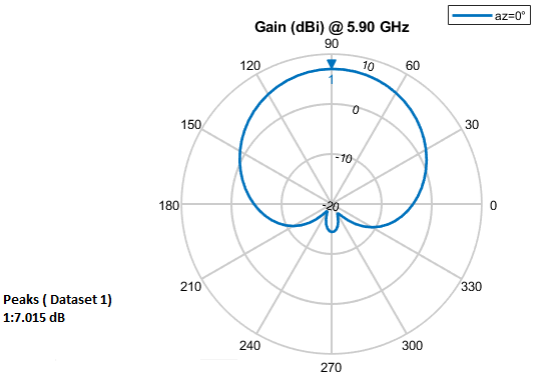

(b)

Fig. 5. Radiation pattern of Microstrip Patch H -Notch antenna, (a). Azimuth radiation pattern; (b). Elevation radiation pattern

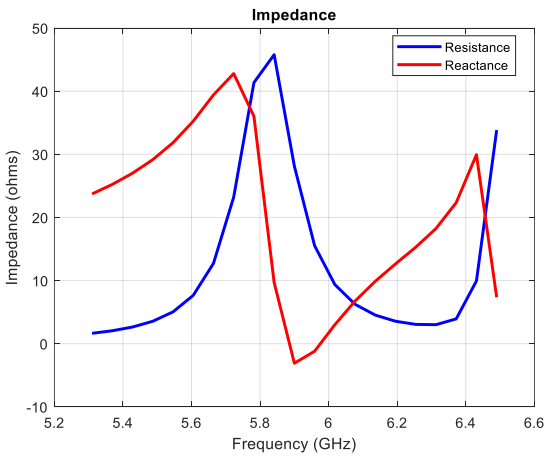

Fig. 6. Impedance verses frequency.

Fig. 6 illustrates that our design antenna is good since the reactance at operating frequency 5.9 GHz (red line) should be zero and the resistance (blue line) should be approximately 50 ohm.

B. Case II

Rectangular Array Patch Microstrip H- Notch antenna element as specification in Table II.

In this work, a unique patch Microstrip H-notch antenna array designed for vehicle communication is investigated.

A low-profile substrate with a relative permittivity of 2.1 and a loss tangent of 0.0002 is used to create the proposed micro strip H-notch antenna array structure with meta-material inspiration. The ground plane length was established using the parametric study and is shown in Fig. 7.

The parameter for antennas with the specified work is covered in Table II.

TABLE II. SIMULATION PARAMETER (PATCH MICROSTRIP H NOTH ANTENNA)

Parameter	Configuration
Rectangular Array size	2 by 2
Row spacing (mm)	25.4
Column Spacing (mm)	25.4
Length of rectangualr array (mm)	17.19
Width of rectangular array (mm)	17.8
Notch Length of rectnagualr array (mm)	3.85
Notch Width (mm)	4.5
Height (mm)	0.933
Ground Plane Length (mm)	25.7
Ground Plane Width (mm)	26.6
Feed Diameter	0.59
Substrate type	Teflon
Epsilone	2.1
Loss Tangent	0.0002
Thkcness of substrate (mm)	0.933
Conductor Type	Copper
Conductivity (S/m)	59600000
Thikness of conductor (mm)	0.0035

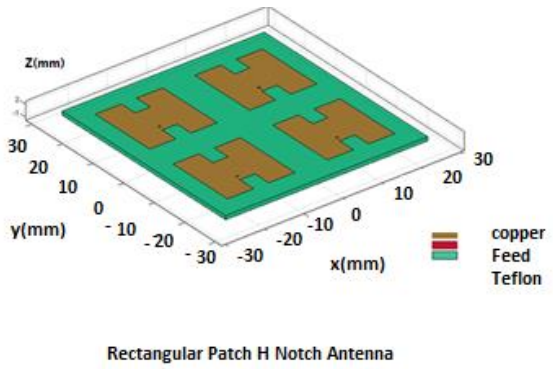

Fig. 7. Structure of Rectangular array of patch microstrip H-notch antenna.

Fig. 8 depicts antenna's radiation pattern. The optimized antenna's increased gain was 11 dBi. The optimized antenna may be categorized as a powerful signal antenna that can broadcast or receive powerful signals in a specific direction due to its greater gain value.

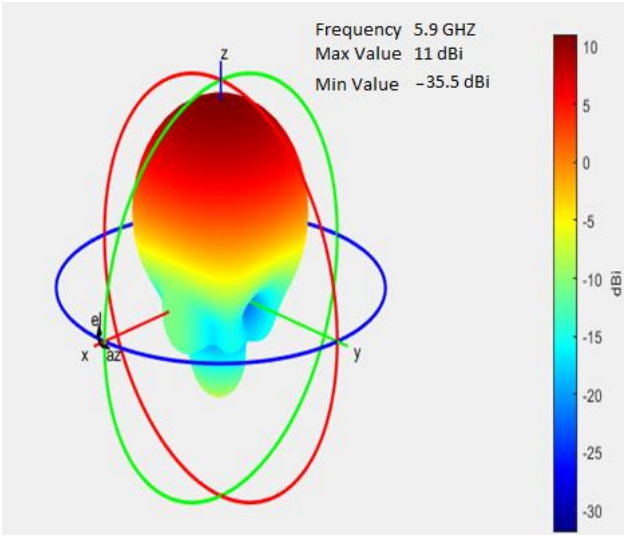

Fig. 8. 3D Radiation pattern.

C. Isolation Characteristics

Since Patch Microstrip H-notch Array antennas are proposed to increase channel capacity, but even the primary performance metric of Patch Microstrip H-notch antenna is the signal correlation of radiation efficiencies, which characterises and enhances the performance and efficiency of the system by reducing the separation between nearby elements, which results in a low correlation between neighbouring antennas. It is possible to observe how the multiple ports on the Patch Microstrip H-notch Array antenna affect mutual coupling by using scattering traits like Sij and Sji. To improve the performance of the antenna, the isolation characteristics should typically be less than 20 dB. When the mutual coupling properties of the nearby regions are compared with the measured findings, it is clear that the simulated and measured results agree in a satisfactory way, as shown in the Fig. 9.

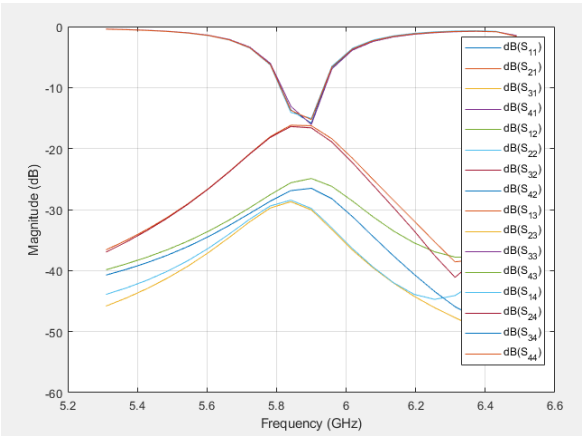

Fig. 9. S Parameters for designed antenna.

The chart above demonstrates that the bandwide isolation characteristics are less than 20 dB. As a result, there is less reciprocal interaction between the elements.

D. Envelope Correlation Coefficient (ECC)

It is critical to calculate the ECC, which illustrates the degree of correlation between various communication channels, in order to evaluate the patch Micro-strip H-notch performance of suggested antennas. The ideal ECC value, according to theory, is zero, although it must be less than 0.5. This value illustrates the relationship between the various antennas at various ports. A lower ECC indicates better antenna performance. A desirable standard value for the hybrid system is ECC 0.5. The two antennas' lower ECC scores show that they are not coupled. The ECC for two adjacent ports is given by [22]

$$\rho_e = \frac{\left|s^*_{11} s_{12} + s^*_{21} s_{22}\right|}{\left(1-\left|s_{11}\right|^2-\left|s_{12}\right|^2\right)\left(1-\left|s_{22}\right|^2-\left|s_{12}\right|^2\right)} \quad (6)$$

where, s_{ij} is the S-parameter of the dual feed antenna, $*$ denotes the complex conjugate operator, $|\cdot|$ is the magnitude operator.

The ECC between the adjacent items is listed in Table III, demonstrating that there is a decreased correlation between them.

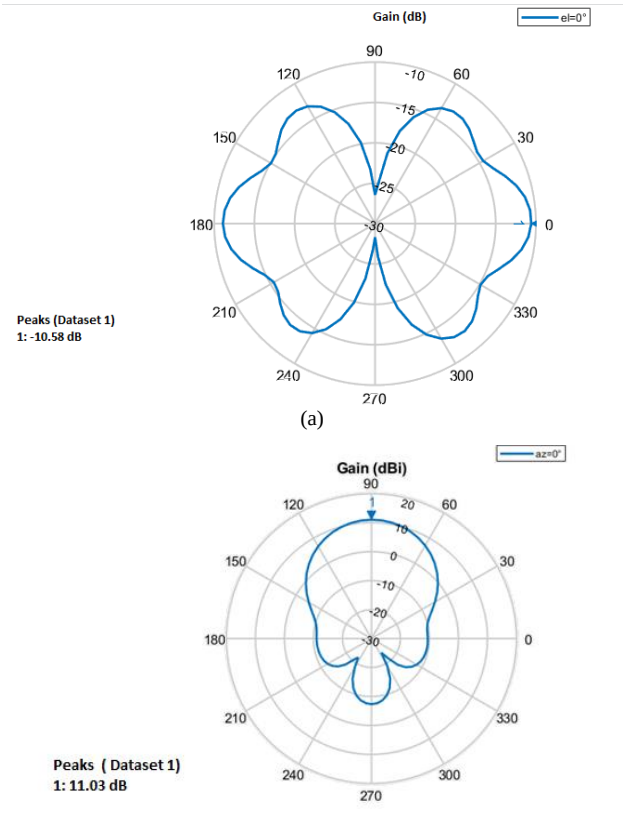

Fig. 10. Measured Gain for the patch Microstrip H-Notch, (a) Azimuth plane pattern at 5.9 GHZ. (b) Elevation plane pattern at 5.9 GHZ.

According to Fig. 10(a), the optimized antenna demonstrated a better azimuth radiation pattern with a main lobe magnitude value of –10.58 dB. A better elevation radiation pattern was demonstrated by the optimized antenna, which had a main lobe magnitude of 11.03 dB as shown in Fig. 10(b).

TABLE III. ECC VALUE ANALYSIS AMONG THE PORTS

Ports	ECG Value
Antenna (1, 2)	0.01
Antenna (1, 3)	0.025
Antenna (1,4)	0.02
Antenna (2, 3)	0.018
Antenna (2, 4)	0.022
Antenna (3, 4)	0.019

IV. RESULTS AND DISCUSSIONS

The low-profile antenna is intended to operate at the vehicular communication-compatible 5.9 GHz resonant frequency. Because Teflon was used as the substrate and a straightforward fabrication procedure was used, this antenna was incredibly affordable to produce. The higher frequency band and the bands' impedance bandwidth were improved by the usage of the Arrays.The suggested antenna's overall size reduction, performance enhancement, and array deployment make it dependable and adaptable for use in vehicle communication settings. These arrays are arranged in an orthogonal packing arrangement to reduce their size, improve isolation between them, and generate a maximum gain of 11 dBi. It demonstrates that the agreement is sound for a driving environment. Simulated results for the S-parameter and radiation pattern at corresponding frequencies are measured. The proposed antenna is built on a single side of premium Teflon substrate and measures just $17.19\times17.8\times0.933$ mm^3. Because it is designed to function at a frequency of 5.9 GHz, it can be used for Internet of Things applications.

In order to improve performance, the individual eleme nts are arranged orthogonally in the array of the microstri p H- notch, resulting in a 4 dB improvement in isolation. For the proposed design, given the specifications, a diversity gain of 11 dB and ECC values of less than 0.05 are obtained. In addition to that, onboard simulation analysis is made and the results were verified. The fundamental Microstrip patch H-notch antenna is first proposed in the study. The performance of the proposed antenna is validated using the return loss and gain characteristics. The maximum gain at 5.9 GHz is 7 dBi, and the return loss value is less than -10 dB. Therefore, it is required to construct an antenna that includes the crucial attributes mentioned above. The sub-6 GHz and millimeter wave frequencies of 5G have emerged as renowned bands of operation in vehicle communication as all other technologies shift to 5G technology for communications. The V2N platform increases traffic efficiency and road safety by establishing communication over an unlicensed 5.9 GHz national information infrastructure.

V. CONCLUSIONS

The two patch antennas that have been presented are each designed to operate in the entire UWB spectrum as well as the specific vehicular communication band. These

antennas were made using a straightforward fabrication technique to increase channel capacity.

The numerous researchers have explored a variety of methods to improve the functionality of Microstrip patch antenna structures, but our suggested construction keeps the array elements orthogonally arranged and closer to one another in order to reduce mutual coupling and improve isolation characteristics. Array Microstrip patch structure performance is evaluated using a number of metrics, including ECC and Radiation patterns.

Diversity techniques increase the number of antennae that must be carried onto the body of the vehicle because there are more places in modern vehicles where antennas can be fitted while employing the diversity approach for the best radio signal reception. It is essential to identify the areas of the car where the antennas can be incorporated in order to prevent damaging the car's aesthetics or any surrounding radiators. To achieve effective diversity performance, the antennas used for diversity reception need to be sufficiently distanced. This suggests that in order to achieve good spatial diversity, the antennas should be at least one wavelength apart. The final suggested antenna is mounted on the vehicle for simulation software study.

Conflict of Interest

The author declares no conflict of interest.

Acknowledgement

The author would like to thank Palestine Technical University Kadoorie (PTUK) for funding this research.

References

[1] S. Akbar, R. Vijay, and S. Ramesh, "Orthogonally integrated hybrid antenna for intelligent transportation systems," *Applied Computational Electromagnetics Society Journal*, vol. 36, no. 5, pp. 519–525, 2022.

[2] H. Alsariera, Z. Zakaria, and A. Isa. "New broadband L-shaped CPW-fed circularly polarized monopole antenna with asymmetric modified ground plane and a couple series-aligning inverted L-shaped strip," *International Journal of Electronics and Communications (AEÜ)*, vol. 118, 2020.

[3] R. Kumar, N. Gupta, and G. Kaur, "Design of wideband CPW fed slotted microstrip patch antenna," *International Journal of Computer Applications*, vol. 108, no. 14, pp. 24–28, 2014.

[4] N. Prabakaran, S. Kaylan, K. Murthy, D. Baba, C. Naveen, and R. Sai, "A coplanar waveguide (CPW) fed circular microstrip antenna for UWB applications," *International Journal of Innovative Technology and Exploring Engineering*, vol. 8, no. 6, pp. 531–534, 2019.

[5] S. Singh, T. Sharan, and A. Singh, "Investigating the S-parameter (|S11|) of CPW-fed antenna using four different dielectric substrate materials for RF multiband applications," *AIMS Electronics and Electrical Engineering*, vol. 6, no. 3, 2024.

[6] P. Boontamchauy, T. Lertwiriyaprapa, and C. Phongcharoenpanich, "Inverted l-shaped CP Patch antenna with corner-truncated partial ground plane diagonally adjoined with square branch for l-band applications," *Sensors*, vol. 21, pp. 1–16, 2021.

[7] J. Yoon, "Rectangular ring open-ended monopole antenna with inverted L-strip for WLAN dual-band operations," *Journal of Information and Communication Convergence Engineering*, vol. 10, no.4, pp. 321–384, 2012.

[8] A. Hossain, M. Islam, M. Chowdhury, and M. Samsuzzman, "A grounded coplanar waveguide-based slotted inverted delta-shaped wideband antenna for microwave head imaging," *IEEE Access*, vol. 8, pp. 185698–185724, 2020.

[9] C. Chiu and M. Y. Chi, "Planar hexa-band inverted-f antenna for portable device applications," *IEEE Antennas and Wireless Propagation Letters*, vol. 8, pp. 1099–1102, 2009.

[10] R. Ma1, Y. Gao, Y. Wang, and C. Parini, "Circular co-planar inverted-f antenna for UHF machine-to-machine communications," *IEEE*, pp. 1418–1419, 2015.

[11] Y. Rahayu and M. Hidayat, "Design of 28/38 GHz dual-band triangular-shaped slot microstrip antenna array for 5G applications," *IEEE*, pp. 93–197, 2018.

[12] L. Anchidin, A. Lavric, P. Mutescu, A. Petrariu, and V. Popa, "The design and development of a microstrip antenna for internet of things applications," *Sensors*, vol. 23, no. 1, pp. 1–14, 2022.

[13] S. Katoch, H. Jotwani, S. Pani, and A. Rajawat, "A compact dual band antenna for IoT applications," in *Proc. International Conference on Green Computing and Internet of Things (ICGCIOT)*, pp. 1954–1597, 2015.

[14] L. Santamaria, F. Ferrero, R. Staraj, and L. Lizzi, "Slot-based pattern reconfigurable ESPAR antenna for IoT applications," *IEEE Transactions on Antennas and Propagation*, vol. 69, no. 7, pp. 3635–3644, 2020.

[15] I. Simanjuntak and A. Kurniawan, "Effect of parasitic patch for the radiation characteristics microstrip antenna planar array with distribution edge," *Journal of Communications*, vol. 18, no. 8, pp. 504–513, 2023.

[16] A. Rajesh, R. Vani, and B. Rao, "Performance analysis of rectangular microstrip wearable textile antenna with series of slots," *Journal of Communications*, vol. 17, no. 5, pp. 365–372, 2022.

[17] A. Alsudani and H. Marhoon, "Design and enhancement of microstrip patch antenna utilizing mushroom like-EBG for 5G communications," *Journal of Communications*, vol. 18, no. 3, pp. 156–163, 2023.

[18] D. Prabhakar, P. Rao, and M. Satyanarayana, "Characteristics of patch antenna with notch gap variations for Wi-Fi applications," *International Journal of Applied Engineering Research*, vol. 11, no. 8, pp. 5741–5746, 2016.

Copyright © 2024 by the authors. This is an open access article distributed under the Creative Commons Attribution License (CC BY-NC-ND 4.0), which permits use, distribution and reproduction in any medium, provided that the article is properly cited, the use is non-commercial and no modifications or adaptations are made.